Paper

A Selective Vision and Landmark based Approach to Improve the Efficiency of Position Probability Grid Localization

Andrey A. Loukianov* Non-member
Masanori Sugisaka* Member

This paper presents a vision and landmark based approach to improve the efficiency of probability grid Markov localization for mobile robots. The proposed approach uses visual landmarks that can be detected by a rotating video camera on the robot. We assume that visual landmark positions in the map are known and that each landmark can be assigned to a certain landmark class. The method uses classes of observed landmarks and their relative arrangement to select regions in the robot posture space where the location probability density function is to be updated. Subsequent computations are performed only in these selected update regions thus the computational workload is significantly reduced. Probabilistic landmark-based localization method, details of the map and robot perception are discussed. A technique to compute the update regions and their parameters for selective computation is introduced. Simulation results are presented to show the effectiveness of the approach.

Keywords: mobile robot, navigation, localization, visual landmarks, probabilistic methods

1. Introduction

Robust and efficient navigation is the key issue in control and operation of autonomous mobile robots [2]. Localization is one of the principal problems in robust navigation, which task is to estimate robot location using sensor data. Reliable and effective localization method has to deal successfully with several issues. It must be able to (1) stably track current robot position, (2) globally locate the robot without prior information on its whereabouts and (3) autonomously recover from errors in position estimation or incorrect previous information. Simple and robust solutions, such as global positioning systems, often conflict with the concept of robot autonomy. A number of methods that can locate the robot without global positioning have been proposed and successfully applied [1][4][9][10].

Probabilistic Markov localization approaches offer a good framework to deal with all the described issues allowing to handle any degree of uncertainty in robot location. The robot's belief about its current posture is represented by a probability density function (PDF) which is spanned over all open environment space and updated by iterative Bayesian *predict-and-match* technique. In the map the location PDF is usually approximated by a 3D probability grid [4] which can grow very large in size for large environments and fine approximation resolution. Therefore, probability grids require large amounts of memory and significant computing power to represent and process them. It makes them inefficient and limits their use in real-time applications. This problem was addressed by several researchers who suggested to use selective computations [4] and dynamic environment representations [3] for general open-space surroundings or effective models for specific environments [9].

Recently, a family of Monte Carlo Localization (MCL) algorithms has become popular [7][10][11]. These methods approximate PDF by the density of weighted point samples distributed in the continuous state space. As the result MCL methods can overcome resolution limitations of Markov localization and can scale their computational requirements by changing sample set size. Nevertheless, MCL algorithms also have limitations. They are very sensitive to the number of samples being used for approximation and to the choice of resampling methods used to update sample sets after movements or sensor readings. The relation between size of environment and required number of samples in MCL is far from obvious and usually has to be determined in experiments. The resampling method may fail to generate or may remove a sample in the right location which will result in robot getting lost. The MCL methods also appear to recover more slowly from unmodelled errors. Therefore the Markov localization is still one of the most robust and powerful localization methods.

This paper presents a selective approach that improves the efficiency of probability grid based Markov localization algorithm without degrading its ability to successfully deal with all the issues of the localization problem. The approach makes use of visual landmarks that can be detected by a rotating video camera on the robot. We assume that the map contains visual landmarks of several distinct classes with known positions. Generally, the vision system can detect and classify landmarks more reliably in contrast to the ultrasonic or range sen-

Department of Electrical and Electronic Engineering, Faculty of Engineering, Oita University,
Dannoharu 700, Oita 870-1192, Japan.

sors which are easily confused in dynamic environments with moving obstacles. Therefore we can avoid the violation of the Markov assumption which states that sensor readings for given state are conditionally independent.

In order to selectively update the posterior location PDF in an efficient way the method uses the information about currently detected landmarks. This information includes combination of recognized classes of detected landmarks and landmarks relative arrangement with respect to the robot. Matching detected landmarks to ones stored in the map allows us to define the regions in the robot posture space for selective computations. The resulting regions take into account the uncertainties in robot perception and map information. Only in these regions the conditional perceptual model is computed and the posterior location PDF is updated on the current matching and the following prediction steps. Thus the computational workload is significantly reduced. When more than one landmarks are detected our approach becomes similar to triangulation localization methods. However it does not require the robot to detect three or more landmarks at a time to localize itself — the probabilistic framework allows the method to make use of any available landmark sightings to refine the robots's belief about its current position.

The paper is organized as follows. Probabilistic landmark-based localization method is reviewed in sections 2 and 3. Section 4 discusses details of the map and robot perception. A technique to compute the update regions and their parameters for selective computation is introduced in section 5. Section 6 presents the results of simulations to show the effectiveness and robustness of the method. In particular, the solutions of the global localization and the so-called "kidnapped robot" problems are presented.

2. Landmark-Based Localization

The mobile robot's location can be defined by the following state vector

$$\boldsymbol{\xi} = [x_p \; y_p \; \vartheta]^T.$$

The environment can be represented as a state space Ξ which spans over all possible robot postures in the given map. The map also contains a set of visual landmarks

$$\mathfrak{L} = \{l_1, \ldots, l_{N_L}\},$$

whose positions in the map are known with given accuracy. Generally, the mobile robot operation can be represented by the sequence of consecutive steps. On t-th step of operation, the robot changes its state by executing a sequence of movements, denoted as a, during which the odometry is used to estimate the relative change in position. Also on t-th step the robot utilizes a video camera to detect a set of landmarks

$$\hat{\mathfrak{L}}_t(\boldsymbol{\xi}) = \{\hat{l}_1, \ldots, \hat{l}_{N_t}\} \subset \mathfrak{L}, \quad 0 \le N_t \le N_L.$$

Each detected landmark is described by some parameters that allow to classify it and to estimate its location relative to the robot. If we assume that the motions and landmark detections are performed in sequence, then the localization problem can be stated in the following general terms:

$$\begin{aligned}&\text{Estimate} \quad \boldsymbol{\xi}_t,\\ &\text{given} \quad \hat{\mathfrak{L}}_t, \hat{\mathfrak{L}}_{t-1}, \ldots, \hat{\mathfrak{L}}_0, \text{ and } a_t, a_{t-1}, \ldots, a_0.\end{aligned}$$

3. Markov Localization Method

According to Markov localization approach the robot's confidence for being at a definite location is expressed by a probability density function $P(\boldsymbol{\xi})$, defined in all state space $\boldsymbol{\xi} \in \Xi$. To obtain a 'true' posture $\boldsymbol{\xi}^*$ one may use an appropriate statistical estimator, such as maximum likelihood estimator

$$\boldsymbol{\xi}^* = \operatorname{argmax}_{\boldsymbol{\xi}} P(\boldsymbol{\xi}). \quad \cdots\cdots (1)$$

The distribution of probability density in $P(\boldsymbol{\xi})$ is conditioned on the history of movements and sensor readings. In other words, $P(\boldsymbol{\xi})$ is estimated recursively by applying Bayes formula with conditional probability distributions calculated for the current motion or sensory data. The sensor readings should satisfy the *Markov assumption* about conditional independence, which, in general, does not hold for dynamic environments with moving obstacles [4].

For each motion on t-th step $P(\boldsymbol{\xi})$ is updated by the following prediction equation

$$P(\boldsymbol{\xi}_t) = \int_{\Xi} P_a(\boldsymbol{\xi}_t|\boldsymbol{\xi}_{t-1}) \, P(\boldsymbol{\xi}_{t-1}) \, d\boldsymbol{\xi}_{t-1}, \quad \cdots\cdots (2)$$

where $P_a(\boldsymbol{\xi}_t|\boldsymbol{\xi}_{t-1})$ is the conditional transition probability for a move a that changed the state by $\Delta\boldsymbol{\xi}$ from previous state $\boldsymbol{\xi}_{t-1}$ to $\boldsymbol{\xi}_t$. Equation (2) is integrated over all previous possible locations $\boldsymbol{\xi}_{t-1}$.

When a set of visual landmarks $\hat{\mathfrak{L}}_t$ is observed $P(\boldsymbol{\xi})$ is updated by the following matching equation

$$P(\boldsymbol{\xi}_t) = \eta \; P(\hat{\mathfrak{L}}_t \,|\, \boldsymbol{\xi}) \; \tilde{P}(\boldsymbol{\xi}_t), \quad \cdots\cdots (3)$$

where $P(\hat{\mathfrak{L}}_t \,|\, \boldsymbol{\xi})$ is the likelihood of observing $\hat{\mathfrak{L}}_t$ conditioned at $\boldsymbol{\xi}$, called sometimes *perceptual model*; $\tilde{P}(\boldsymbol{\xi}_t)$ is the prior probability density and $\eta = |\sum_{\Xi} P(\boldsymbol{\xi}_t)|^{-1}$ is the normalization factor.

4. The Map and Robot Perception

In Markov localization the state space (map) is usually represented by a 3D position probability grid which piecewise approximates $P(\boldsymbol{\xi})$, though more complex and dynamic representations also can be adopted [3]. In this paper we use the probability grid representation superposed by a 2D logical occupancy grid of the same resolution.

In our method we use visually detectable landmarks. Each visual landmark has known map coordinates $\boldsymbol{p} = [x_l \; y_l]^T$. Any environment feature (natural or artificial) can represent a visual landmark if it can be captured by a video camera and reliably recognized. Robust and reliable recognition of the visual landmark in a video image helps to avoid the violation of the Markov assumption for dynamic environments.

In order to fully utilize the landmark-based localization the environment should contain many visual landmarks. Some of the proposed methods rely on the assumption that all landmarks are distinguishable [1]. In practice, when the number of landmarks is large it is very difficult to make all of them unique. Here we assume that each landmark can be attributed to a separate class of landmarks $l_i \in \mathfrak{L}_k$. One landmark can belong only to one class and within each class the landmarks are indistinguishable. These assumptions result in the following conditions:

$$\mathfrak{L} = \mathfrak{L}_1 \cup \mathfrak{L}_2 \cup \ldots \cup \mathfrak{L}_{N_K},$$

$$0 = \mathfrak{L}_1 \cap \mathfrak{L}_2 \cap \ldots \cap \mathfrak{L}_{N_K}.$$

Landmark classes correspond to various types of landmarks: markers of certain shape or color, stationary objects (door frames, corners, power sockets), etc. There is a variety of image processing methods to accomplish recognition and classification tasks. Selection of these methods is not the focus of this paper. So each landmark in the map is described as $l_i = \{\boldsymbol{p}_i,\ \mathfrak{L}_k\}$.

To detect landmarks we propose to use a conventional video camera with pan-tilt capabilities. Each detected landmark $\hat{l}_j$ is described by the following parameters $\hat{l}_j = \{\hat{\boldsymbol{b}}_j,\ \mathfrak{L}_m\}$, where $\hat{\boldsymbol{b}}_j = [r_j\ \tau_j]^T$ are estimated polar coordinates (distance and bearing angle) of the landmark with respect to the robot. In order to estimate relative position of the landmark using a single camera we propose to enforce the condition for landmark placement which will give necessary depth information. The condition is that all landmarks of the same class should be located at the same height above floor level. This condition can be easily assured in practice since positions of most salient features of indoor environment usually comply with it. For more accurate measurement the optical and kinematic parameters of the rotating camera have to be determined through a calibration procedure [6].

As in the real world, we consider the robot perception and environment map to have some errors and inaccuracies. Here we assume that these errors may be represented by zero-mean normal distributions. The landmark position $\boldsymbol{p}$ in the map is given with accuracy expressed by a variance σ_l^2 and corresponding covariance matrix $\boldsymbol{C}_l = \sigma_l^2 \boldsymbol{I}^{2\times 2}$. The relative position $\hat{\boldsymbol{b}}$ of observed landmark is estimated with accuracy expressed by a covariance matrix $\hat{\boldsymbol{C}}_b = \mathrm{diag}[\sigma_r^2\ \sigma_\tau^2]$. The estimation error may be introduced by the noise in visual system, the imperfections in environment and landmarks. This error is usually modelled using the statistical data collected from the sensory system. In our paper we assume that distance measurement error σ_r^2 linearly depends on r, and the angular measurement error σ_τ^2 is constant.

5. Selective Computation Approach

To improve the computational efficiency of Markov localization one may use selective computation techniques. A straightforward way is to set a minimal probability

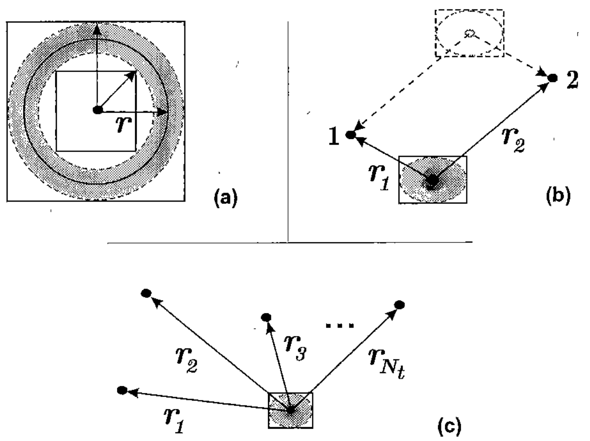

Fig. 1. Examples of update regions (2D projections).

threshold for the grid cell to be updated in Eqs. (2) and (3). This trivial approach saves some computations but also have some pitfalls. The first is that each state has to be accessed at least once on every iteration anyway to check for the threshold condition. The second, more important, drawback is that ignoring prior states with low probability may deteriorate the method's ability to recover from localization and measurement errors. When these errors are finally detected in sensor matching step then the minimal probability threshold may force the method to switch to time consuming global localization (when the robot cannot normally operate) instead of considering other states with low probability that possibly correspond to a true location. This case is illustrated in our simulation of the kidnapped robot problem.

In our selective approach we suggest establishing geometrical constraints which will specify possible areas in the state space where the location PDF is updated in (2) and (3). To define the areas, which we call the *update regions*, we match the set of detected landmarks to the landmarks stored in the map. Landmarks types and their relative arrangement are used in the matching process. The update regions are attached to the matched groups of landmarks and mapped into discrete state space represented by a probability grid. Only the discrete states that are spanned by one or more update regions are accessed by update algorithms. The examples of such update regions for one (a), two (b) and multiple (c) observed landmarks are shown in Fig. 1 as 2D projections into 3D state space (the actual update regions are three-dimensional). This approach is somewhat similar to the one described in [11] which employed landmark-robot relative poses to track multiple location hypotheses in landmark-attached reference frames using MCL.

The process of selecting map landmarks that match detected ones is described as follows. When a single landmark is detected the update regions similar to Fig. (1a) are simply attached to all landmarks of the same type as the detected one. For two or more detected landmarks the combination of their types and the distance measure between their pairs are used to se-

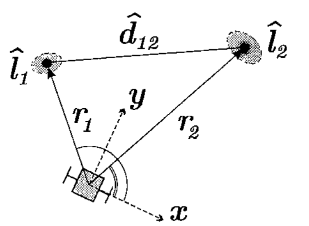

Fig. 2. The pair of detected landmarks.

lect similar landmarks from the map. Information about pairs of map landmarks is stored in the precomputed index which includes combination of their types $\{\mathfrak{L}_i, \mathfrak{L}_j\}$, distance $d = \|\boldsymbol{p}_i - \boldsymbol{p}_j\|$ and its variance $\sigma_d^2 = \sigma_{li}^2 + \sigma_{lj}^2$. The index includes every pair of landmarks for which the condition $d < 2r_{max}$ is true, where r_{max} is the maximal perceptual range of the robot. For each pair of detected landmarks (Fig. (2)) the same parameters are computed: types combination, distance $\hat{d}$ and distance variance $\hat{\sigma}_d^2$. To compute these parameters the landmark polar coordinates $\hat{\boldsymbol{b}}_i$ and their uncertainties $\hat{\boldsymbol{C}}_{bi}$ are converted to the robot local cartesian frame. The uncertainty in measured distance $\hat{\sigma}_d^2$ is estimated by adding measurement errors in robot cartesian frame and projecting the result into the line connecting both detected landmarks, namely

$$\hat{\sigma}_d^2 = \sum_i (\sigma_{ri}^2 \cos^2(\theta - \tau_i) + r_i^2\, \sigma_{\tau i}^2 \sin^2(\theta - \tau_i)), \quad (4)$$

where θ is the angle between the line connecting two landmarks and X axis of the robot reference frame. The candidate pairs of map landmarks are selected by matching landmark types, similarity criteria $S < S_{max}$ condition and pair combinations. The matching similarity criteria S for a pair is calculated as

$$S = \frac{|d - \hat{d}|}{\sqrt{\sigma_d^2 + \hat{\sigma}_d^2}}. \quad \cdots\cdots\cdots\cdots\cdots\cdots\cdots\cdots\cdots (5)$$

Each update region is defined by its center and size. The size is defined by the uncertainty resulted from measurement errors and map inaccuracies. This uncertainty is expressed by covariance matrix $\boldsymbol{C}_r$. In single landmark case the update region center coincides with a landmark and the uncertainty $\boldsymbol{C}_r \in R^{2\times 2}$ is best computed in polar reference frame attached to the landmark as

$$\boldsymbol{C}_r = \hat{\boldsymbol{C}}_b + \boldsymbol{J}\,\boldsymbol{C}_l\,\boldsymbol{J}^T, \quad \cdots\cdots\cdots\cdots\cdots\cdots\cdots (6)$$

where $\boldsymbol{J} = \partial \boldsymbol{b}/\partial \boldsymbol{p}^T$ is the jacobian transformation matrix. This covariance matrix defines the 'thickness' of the hollow square in Fig. (1a) and the width of distribution in ϑ dimension.

In other cases the center of update region $\boldsymbol{p}_r$ is computed using triangulation techniques [1]. The uncertainty in position of the center and the size of the region are expressed by $\boldsymbol{C}_r \in R^{3\times 3}$, which is computed in cartesian reference frame as

$$\boldsymbol{C}_r = \sum_{i=1}^{N_t} \left(\boldsymbol{J}_{bi}\,\hat{\boldsymbol{C}}_{bi}\,\boldsymbol{J}_{bi}^T + \boldsymbol{J}_{pi}\,\boldsymbol{C}_{li}\,\boldsymbol{J}_{pi}^T \right), \quad \cdots\cdots (7)$$

where $\boldsymbol{J}_{bi} = \partial \boldsymbol{p}_r/\partial \boldsymbol{b}_i^T$ and $\boldsymbol{J}_{pi} = \partial \boldsymbol{p}_r/\partial \boldsymbol{p}_i^T$. The actual size of regions is computed from $\boldsymbol{C}_r$ using preset value of maximum standard deviation for normal distribution.

Before updating the location PDF in Eq. (3) the conditional probability distribution $P(\hat{\mathfrak{L}}|\boldsymbol{\xi})$ has to be computed. First, the probability distribution is calculated for each update region using the following formulas: for single landmark

$$p(\hat{\mathfrak{L}}|\boldsymbol{\xi}) = \phi_2\left(\Delta \boldsymbol{b}, \boldsymbol{C}_r\right), \quad \cdots\cdots\cdots\cdots\cdots\cdots\cdots (8)$$

otherwise

$$p(\hat{\mathfrak{L}}|\boldsymbol{\xi}) = \phi_3\left(\Delta \boldsymbol{p}_r, \boldsymbol{C}_r\right), \quad \cdots\cdots\cdots\cdots\cdots\cdots\cdots (9)$$

where ϕ_2 and ϕ_3 are the 2D and 3D Gaussian distributions defined in polar and cartesian reference systems, respectively. The overall conditional perceptual model for given location $\boldsymbol{\xi}$ is defined by the expression

$$P(\hat{\mathfrak{L}}|\boldsymbol{\xi}) = 1 - \prod_{N_u} \left(1 - p(\hat{\mathfrak{L}}|\boldsymbol{\xi})\right), \quad \cdots\cdots\cdots\cdots (10)$$

where N_u is the number of update regions that include the location $\boldsymbol{\xi}$ in 3D space.

Since $P(\hat{\mathfrak{L}}|\boldsymbol{\xi})$ is zero outside update regions the result of Eq. (3) is also zero in these locations. Therefore the location PDF needs to be updated in the matching step only in locations spanned by at least one update region in the map. Locations outside any of update regions in the probability grid are assumed to have zero probability and not accessed by the algorithm. It is important to mention that the prior probability $\tilde{P}(\boldsymbol{\xi}_t)$ in Eq. (3) in our update algorithm implementation is assumed to have very low background noise that is larger that zero. In our case we set this value to 0.01 of the uniform PDF in Ξ. This assumption does not affect the normal operation but helps to reset the posterior PDF to the most recent sensor reading if (a) the observation is completely not supported by prior information ('kidnapped' robot problem) or (b) the observation error falls out of predicted range due to unmodelled errors. This resetting is performed automatically when the is normalization factor η is computed in the end of update cycle.

On the next $(t+1)$ iteration the same update regions are used to selectively designate possible locations of $\boldsymbol{\xi}_{t-1}$ for the prediction step in update equation (2). Therefore using update regions in those equations can significantly reduce the overall computational workload.

5.1 Summary of the Algorithm

Movement update:

- apply Eq. (2) to all locations $\boldsymbol{\xi}_{t-1}$ that are inside update regions calculated on the previous $(t-1)$ step.

Sensor update:

- match detected landmarks to map landmarks and select candidate combinations;
- for every region compute $\boldsymbol{p}_r$ and $\boldsymbol{C}_r$, and map the region into the discrete state space coordinates (probability grid);
- compute a perceptual model $p(\hat{\mathfrak{L}}|\boldsymbol{\xi})$ in each region and join them into the overall distribution $P(\hat{\mathfrak{L}}|\boldsymbol{\xi})$.

- apply Eq. (3) to all locations inside update regions. If $\tilde{P}(\boldsymbol{\xi}_t) = 0$, set $\tilde{P}(\boldsymbol{\xi}_t) = 0.01/N_{\Xi}$, where N_{Ξ} is the total number of states.
- compute normalization factor η.

6. Simulation Results

To test the robustness and efficiency of the proposed approach two simulations of different localization problems were performed. The global and the so-called 'kidnapped robot' localization problems were considered.

The robot's motions are modelled to be inexact, so the uncertainty related to the location predicted by odometry is growing along the course of motion. The odometry position uncertainty is expressed by the covariance matrix $\boldsymbol{C}_a \in R^{3\times 3}$ which is continuously updated by low-level robot controller during the move a. The update technique is similar to the one described by Crowley [(5)]. The accumulated uncertainty $\boldsymbol{C}_a$ at the end of the move a is used to compute conditional transition probability $P_a(\boldsymbol{\xi}_t|\boldsymbol{\xi}_{t-1})$ in Eq. (2) using the following expression

$$P_a(\boldsymbol{\xi}_t|\boldsymbol{\xi}_{t-1}) = \phi_3\left(\Delta\boldsymbol{\xi}, \boldsymbol{C}_a\right), \quad \cdots\cdots\cdots\cdots\cdots\cdots (11)$$

where ϕ_3 is 3D Gaussian distribution.

The map in simulations had size 15×12.5 m and contained three indistinguishable visual landmarks of the same class. The landmarks positions were known with limited accuracy: $\sigma_{l1}^2 = 0.08$ m^2, $\sigma_{l2}^2 = 0.03$ m^2, $\sigma_{l2}^2 = 0.1$ m^2. The map was represented by a probability grid with linear resolution of 0.25 m and angular resolution 15° totaling to 72000 possible states. In both simulations the mobile robot was able to detect only one landmark at a time, so the area of update regions was the largest possible (see Fig. 1).

In the first simulation the proposed method was used to solve the global localization problem which is to estimate robot location in the map without knowing initial position. The results of simulation in progress for this problem are shown in Fig. 3. In this and next figures the 2D projections of location probability density function $P(\boldsymbol{\xi})$ are shown, where darker areas correspond to robot locations with higher probability. The actual location of the robot is shown by the crossed circle. The approach took four steps (four moves and observations) to converge. During its movements the robot observed a sequence of landmarks (#1, #2, #3), one at a time. First two figures show robot's location belief after initial observation and the first movement with landmark #1 in sight. The rightmost figure show computed robot position after fourth step when landmark 3 was sighted. On average only 5.3 % of all states were accessed and updated.

Simulation results for the so-called 'kidnapped robot' localization problem are shown in Fig. 4. In this case the robot is intentionally subjected to localization error to test the ability of the method to recover from it. The robot believes that it is perfectly localized but his location belief is wrong (see left Fig. 4). The actual robot's path in this simulation is intentionally chosen to be ambiguous as a mirror reflection of robot's believed path with respect to landmarks #2 and #3. Since these landmarks are of the same class the robot cannot tell the difference between them. This makes the robot think that his incorrect location is true for some time (middle figure - landmark #2 is sighted and misinterpreted as landmark #3). Only when the unexpected landmark #1 is detected the method abandons its previous wrong location and finds a true location after one update of posterior in Eq. (3) (right figure). This was possible because the approach kept track of another probable location estimate that resulted from previous observations along the path. When the robot was deceived by the ambiguous sensor data on first steps and the alternative location had very small probability that could be neglected if the minimal probability threshold was used. But when the robot had received new sensor data that completely did not match prior location estimate the low probability guess was automatically brought from background by normalization as a second best estimate. Here it took five steps to converge the estimated posture to the true one. On average only 5.6 % of all states were accessed and updated in (2) and (3).

7. Conclusion

In this paper we presented a selective vision and landmark based approach to improve the effectiveness of Markov localization with probability grid approximation. The approach uses visually detectable landmarks that are distinguishable only by their types. Landmarks of the same type are undistinguishable. A detected landmark is described by corresponding landmark type and its coordinates relative to the robot. A map landmark is described by its type, location in the map, and location uncertainty.

The efficiency is achieved by selectively updating the probability grid only inside estimated update regions defined in the state space. The update regions are attached to the landmarks in the map that are similar to the detected ones. The number of update update regions and their placement are decided by matching the set of detected landmarks to the set of map landmarks using types of detected landmarks and their relative arrangement with respect to the robot. The size of update regions is determined by fusing the coordinate uncertainties of matched map landmarks with the errors in estimating detected landmarks positions.

The update equations are applied only in these update regions in the map state space on the current matching and the following prediction iterations steps. Thus the computational workload is significantly reduced. The results of simulations show that the approach is effective and is able to solve all range of issues in the localization problem, including global localization and recovery from localization errors.

(Manuscript received March 18, 2002, revised October 25, 2002)

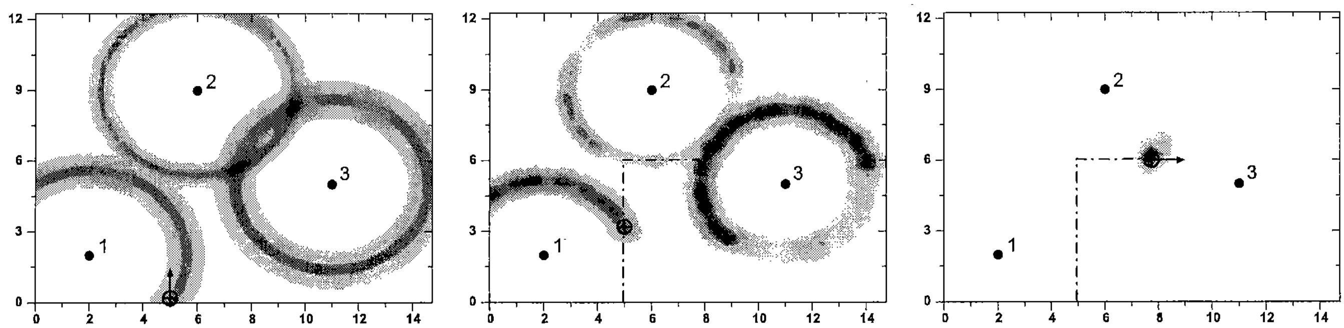

Fig. 3. Global localization problem simulation.

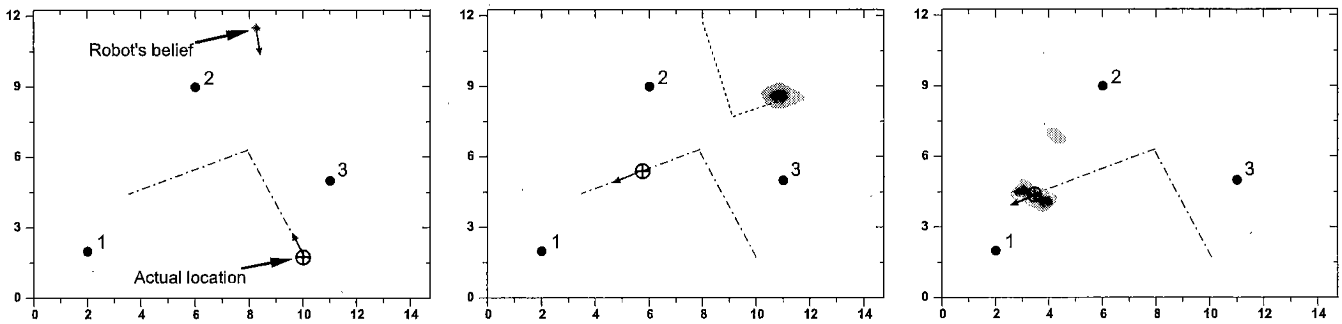

Fig. 4. 'Kidnapped robot' localization simulation.

References

(1) M. Betke and L. Gurvits: "Mobile robot localization using landmarks", In *Proc. of the IEEE Int. Conf. on Robotics and Automation*, pp. 135–142 (1994)

(2) J. Borenstein, et al.: *Navigating Mobile Robots: Systems and Techniques*, A. K. Peters, Ltd, (1996)

(3) W. Burgard, et al.: "Integrating global position estimation and position tracking for mobile robots: The dynamic markov localization approach", In *Proc. of Int. Conf. on Intelligent Robots and Systems*, (1998)

(4) W. Burgard, et al.: "Position tracking with position probability grids", In *Proc. of 1st Workshop on Advanced Mobile Robots* (1996)

(5) J. L. Crowley: "Mathematical foundations of navigation and perception for an autonomous mobile robot", In *Proc. of The Workshop on Reasoning With Uncertainty in Robotics*, pp. 9–51 (1995)

(6) J. Heikkilä and O. Silvén: "Calibration procedure for short focal length off-the-shelf CCD cameras", In *Proc. of 13th Int. Conf. on Pattern Recognition*, Austria, pp. 166–170 (1996)

(7) S. Lenser and M. Veloso: "Sensor resseting Localization for Poorly Modelled Mobile Robots", In *Proc. of Int. Conf. on Robotics and Automation*, pp. 1225–1232 (2001)

(8) A. A. Loukianov and M. Sugisaka: "A Hybrid Method for Mobile Robot Probabilistic Localization Using a Single Camera", In *Proceedings of Int. Conf. on Control, Automation and Systems*, Korea, pp. 280–283 (2001)

(9) S. Thiebaux and P. Lamb: "Combining kalman filtering and markov localization in network-like environments," In *Pacific Rim Int. Conf. on Artif. Intelligence*, pp. 756–766 (2000)

(10) S. Thrun, et al.: "Robust monte carlo localization for mobile robots", In *Artif. Intelligence* 128:1-2, pp. 99–141 (2001)

(11) M. Tomono and S. Yuta: "Mobile Robot Localization based on an Inaccurate Map", In *Proc. of Int. Conf. on Intelligent Robots and Systems*, pp. 399–405 (2001)

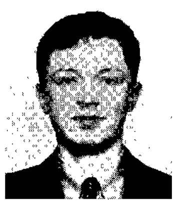

Andrey A. Loukianov (Non-member) was born in Irkutsk, Russia in 1973. He received the M.S. Eng. degree in Electrical Engineering from Irkutsk State Technical University in 1995. He received the D. Eng degree from Laboratory of Automation of Laser Physics Institute, Russian Academy of Sciences in 1999. His research interests include intelligent robotics, mobile robots and numerical analysis and control of nonlinear systems.

Masanori Sugisaka (Member) He received the D. Eng. degree in Electrical Engineering from Kyushu University in 1975. From 1973 to 1974, he was research associate at Oita University. Since 1988, he has been a professor at Oita University. Now he belongs to the Graduate School of Electrical and Electronic Engineering, Oita University. His current research interests are in the fields of artificial life and robotics, especially artificial brain. He is a member of the Institute of Electrical Engineers of Japan, a member of SICE and a member of IEEE.